Atmos. Chem. Phys., 11, 11055–11067, 2011
www.atmos-chem-phys.net/11/11055/2011/
doi:10.5194/acp-11-11055-2011

Atmospheric Chemistry and Physics

Volatility of secondary organic aerosol during OH radical induced ageing

K. Salo[1], M. Hallquist[1], Å. M. Jonsson[1,2], H. Saathoff[3], K.-H. Naumann[3], C. Spindler[4], R. Tillmann[4], H. Fuchs[4], B. Bohn[4], F. Rubach[4], Th. F. Mentel[4], L. Müller[5], M. Reinnig[5], T. Hoffmann[5], and N. M. Donahue[6]

[1]Atmospheric Science, Department of Chemistry, University of Gothenburg, Sweden
[2]IVL Swedish Environmental Research Institute, Sweden
[3]Institute for Meteorology and Climate Research, Karlsruhe Institute of Technology (KIT), Germany
[4]Institut fur Energie- und Klimaforschung, IEK-8, Forschungszentrum Jülich GmbH (FZJ), Germany
[5]Institut für Anorganische und Analytische Chemie, Johannes Gutenberg-Universität, Mainz, Germany
[6]Center for Atmospheric Particle Studies, Carnegie Mellon University, Pittsburgh, USA

Received: 14 June 2011 – Published in Atmos. Chem. Phys. Discuss.: 7 July 2011
Revised: 26 October 2011 – Accepted: 26 October 2011 – Published: 9 November 2011

Abstract. The aim of this study was to investigate oxidation of SOA formed from ozonolysis of α-pinene and limonene by hydroxyl radicals. This paper focuses on changes of particle volatility, using a Volatility Tandem DMA (VTDMA) set-up, in order to explain and elucidate the mechanism behind atmospheric ageing of the organic aerosol. The experiments were conducted at the AIDA chamber facility of Karlsruhe Institute of Technology (KIT) in Karlsruhe and at the SAPHIR chamber of Forchungzentrum Jülich (FZJ) in Jülich. A fresh SOA was produced from ozonolysis of α-pinene or limonene and then aged by enhanced OH exposure. As an OH radical source in the AIDA-chamber the ozonolysis of tetramethylethylene (TME) was used while in the SAPHIR-chamber the OH was produced by natural light photochemistry. A general feature is that SOA produced from ozonolysis of α-pinene and limonene initially was rather volatile and becomes less volatile with time in the ozonolysis part of the experiment. Inducing OH chemistry or adding a new portion of precursors made the SOA more volatile due to addition of new semi-volatile material to the aged aerosol. The effect of OH chemistry was less pronounced in high concentration and low temperature experiments when lower relative amounts of semi-volatile material were available in the gas phase. Conclusions drawn from the changes in volatility were confirmed by comparison with the measured and modelled chemical composition of the aerosol phase. Three quantified products from the α-pinene oxidation; pinonic acid, pinic acid and methylbutanetricarboxylic acid (MBTCA) were used to probe the processes influencing aerosol volatility. A major conclusion from the work is that the OH induced ageing can be attributed to gas phase oxidation of products produced in the primary SOA formation process and that there was no indication on significant bulk or surface reactions. The presented results, thus, strongly emphasise the importance of gas phase oxidation of semi- or intermediate-volatile organic compounds (SVOC and IVOC) for atmospheric aerosol ageing.

Correspondence to: K. Salo
(kent.salo@chem.gu.se)

1 Introduction

Atmospheric aerosol particles are of importance both for human health effects and the effect on the climate by direct and indirect influence on the radiation budget. One significant source of aerosol particles is the gas-to-particle conversion of volatile organic compounds (VOC) induced by atmospheric oxidation, i.e. secondary organic aerosols (SOA) (Hallquist et al., 2009). Many modelling, field and laboratory studies on SOA have been conducted during the last few years e.g. Andreae et al. (2009), Hallquist et al. (2009), Jimenez et al. (2009), Saathoff et al. (2009) and Ng et al. (2010). However, there are still areas of large uncertainty, especially regarding the oxidation steps of the initial precursor molecules and the actual identification and properties of products formed in these processes (Kroll et al., 2008). These reactions and the properties of the resulting aerosols are of concern for the atmospheric ageing processes of SOA and are linked to both condensed and gas phase processes (Jimenez et al., 2009; Donahue et al., 2011; Kroll et al., 2011). Consequently, the term SOA ageing is a change of SOA properties with time and corresponding ageing processes may take place both in gas and condensed phase.

Published by Copernicus Publications on behalf of the European Geosciences Union.

The initial reaction producing SOA is the oxidation of organic compounds by ozone, hydroxyl or nitrate radicals. The ozone reaction is important to the overall SOA formation from unsaturated compounds (Jonsson et al., 2006; Johnson and Marston, 2008). This takes places via an addition of ozone to the carbon-carbon double bond leading to formation of a primary ozonide that quickly splits, producing a carbonyl moiety and a carbonyl oxide known as a Criegee Intermediate (CI). The CI will react further to produce the first generation of stable products. These can be found both in the condensed and gaseous phase depending on their saturation vapour pressures (Pankow, 1994). For unsaturated compounds with the double bond within a ring structure (endocyclic alkenes), ozonolysis is an effective way to increase the oxygen to carbon ratio and polarity without fragmentation of the parent compound.

In the atmosphere, during daytime, the subsequent oxidation of ozonolysis products will most likely occur via reaction with the OH radical. The OH radical reacts with saturated VOCs by hydrogen abstraction, which forms a water molecule and an alkyl radical. This is followed by the fast addition of O_2 to form peroxy radicals. The radicals formed in these reactions will take part in further reactions to form a wide array of products in the atmosphere. The OH radical reaction with organic compounds in the gas phase often occurs within an order of magnitude of the diffusion limit. As outlined by Lambe et al. (2009) the heterogeneous reaction of OH radicals with the SOA particles should be slower by more than an order of magnitude than the homogeneous reactions with the gas phase of the aerosol.

It is not fully clear how fast OH reactions proceed in the SOA condensed phase (George and Abbatt, 2010) however, recent laboratory studies indicate the possibility of oxidation, accelerated by photo-sensitized reactions (D'Anna et al., 2009). In the condensed phase the reaction may be mass-transport limited. For example, SOA may form a viscous liquid or an amorphous solid state that significantly reduces the liquid phase diffusion (Zobrist et al., 2008; Buchholz, 2010; Virtanen et al., 2010). That would probably confine OH reactions to an outer shell of the particles.

Generally, one may divide oxidation products by ozonolysis or by OH reactions with respect to volatility as: intermediate-volatile (IVOC) – found predominately in the gas phase; semi-volatile (SVOC) present both in gas and condensed phase and low-volatile (LVOC) predominately in the condensed phase (Donahue et al., 2009). Clearly atmospheric ageing of SOA aerosol particles takes place but it may happen either via gas phase oxidation with subsequent condensation or via surface/bulk phase reactions. It has been postulated but not yet proved that selected larger more oxidised SOA constituents may significantly fragment into more volatile compounds with time, i.e. any oxidation of organics will eventually produce H_2O and CO_2 (Kroll and Seinfeld, 2008; Jimenez et al., 2009; Kroll et al., 2011).

The work presented herein was part of The MUltiple Chamber Aerosol Chemical Ageing Study, or MUCHACHAS campaign (Donahue et al., 2011). The present paper is based on data from two simulation chamber facilities, the AIDA chamber of Karlsruhe Institute of Technology (KIT) in Karlsruhe (Saathoff et al., 2009) and the SAPHIR chamber of Forchungzentrum Jülich (FZJ) in Jülich (Rohrer et al., 2005; Schlosser et al., 2009). The overall MUCHACHAS campaign includes two additional chambers, at the Paul Scherrer Institute (PSI) (Tritscher et al., 2011) and the Carnegie Mellon University (CMU) chambers (Presto and Donahue, 2006). A sequence of complementary experiments was designed in accordance with the respective chamber attributes. The common objective was to investigate how oxidation chemistry induced by OH radicals change mass concentrations and properties of a secondary organic aerosol produced from ozonolysis of α-pinene and/or limonene (Donahue et al., 2011). The results presented in this work focus on the thermal properties of the aerosol particles, i.e. the volatility obtained by a Volatility Tandem Mobility Analyser (VTDMA). The VTDMA technique (Rader and McMurry, 1986) is a robust and reliable method to probe physical properties such as saturation vapour pressures and enthalpies of sublimation/evaporation e.g. Salo et al. (2010) with references. It has also been used to follow changes in thermal properties of SOA induced by changes in chemical composition (Kalberer et al., 2004; An et al., 2007; Jonsson et al., 2007). The results are discussed in relation to complementary data, changes in the chemical composition and the oxidation processes.

2 Experimental

2.1 Experimental set-up

The AIDA and SAPHIR chambers used in this study have been used for SOA research in several previous studies and are only briefly described here.

The large aerosol and cloud simulation chamber facility AIDA (Aerosol Interaction and Dynamics in the Atmosphere) recently hosted an extensive study on the temperature effect of SOA formation from α-pinene and limonene (Jonsson et al., 2007; Saathoff et al., 2009; Tillmann et al., 2010) and is described in detail in Saathoff et al. (2003, 2009). The AIDA chamber consists of an aluminium vessel of 84.5 m^3 in which temperature (183–333 K) and pressure (0.01–1000 hPa) can be set and controlled precisely. For MUCHACHAS experiments in AIDA, OH radicals were generated in the dark by ozonolysis of tetramethyl-ethylene (TME) with an excess of ozone (Lambe et al., 2007).

The SAPHIR (Simulation of Atmospheric PHotochemistry In a large Reaction chamber) facility has been used for low concentration experiments with focus on understanding photochemistry of the troposphere e.g. Rohrer et al. (2005)

and recently also been used for aerosol formation studies e.g. Rollins et al. (2009). The SAPHIR atmosphere simulation chamber is a 270 m^3 double walled fluorinated ethylene-propylene (FEP) outdoor photo-reactor suitable for OH production using natural sunlight, e.g. photolysis of O_3, HONO or H_2O_2.

A VTDMA set-up, as described by Jonsson et al. (2007), was used to determine the thermal characteristics of organic aerosol particles generated from the ozonolysis reaction of α-pinene and limonene. The aerosol was sampled from the chambers using 6 mm stainless steel tubing, equilibrated to ambient temperature and finally dried using a Nafion drier (Perma Pure PD50-12). A narrow size range was selected using a Differential Mobility Analyser (DMA) operated in a recirculating mode. Typically, the initial mean particle diameters selected were between 50 and 130 nm depending on the dynamics of the aerosols in the chambers, i.e. the particles grow during an experiment. The size selected aerosol was subsequently directed under laminar flow conditions through one of the eight heated parallel tubes in the conditioning oven unit. The heated part of each of the ovens consists of a 50 cm stainless steel tube mounted in an aluminium block with a heating element. The temperature was controlled and monitored with eight temperature sensors and controllers (Pt 100, Hanyoung MX4). The temperatures of each of the eight tubes could be set independently from 298 to 573 K to enable swift changes in evaporative temperatures by switching the flow between the ovens. With a sample flow of 0.3 LPM a residence time of 2.8 s (at 298 K) in the heated part of the oven was achieved. At the exit of the heated part, the evaporated gas was adsorbed by activated charcoal diffusion scrubbers in order to prevent re-condensation. The resulting aerosol was classified using an SMPS (TSI 3096). The final particle mode diameter (D_f) after evaporation was monitored for a number of temperature settings and normalised to the initial particle mode diameter (D_i) determined after the aerosol passed the oven while held at the reference temperature (298 K). The Volume Fraction Remaining (VFR) was determined as $VFR = (D_f)/(D_i)^3$, assuming spherical particles. This procedure was used to ensure that any changes in D_p was a result of evaporation in the oven unit and to avoid artefacts from possible evaporation in the sampling lines. The use of this procedure also improves the reproducibility of experimental results (Jonsson et al., 2007). During an experiment two types of volatility data sets were obtained. The general changes in volatility as a function of time were obtained at a constant evaporative temperature, e.g. 383 K denoted as VFR (383 K). At selected occasions detailed thermal characterisation was done via collection of a so-called thermogram. A thermogram consists of measurements of the VFR over an extended range of temperatures from 298 up to 573 K; a thermogram with ten temperatures takes approximately 40 min to obtain.

During the campaigns both chambers were equipped with a suite of instruments to follow changes in concentrations and properties of both the gas and the particulate phase. To detect gas-phase organic compounds with a time resolution of 5 min, a high-sensitivity Proton Transfer Reaction-Mass Spectrometer was used (PTR-MS, IONICON, Innsbruck, Austria) (Lindinger et al., 1998). The PTR-MS measured SOA precursors and products but also selected organic tracer compounds to determine the OH concentrations. The PTR-MS drew samples from the AIDA chamber via a stainless steel tube (4 mm inner diameter; ID) through a Teflon filter (PTFE, 0.2 µm pore size, Satorius) located in the thermostated housing. The filter could also be bypassed. It removed aerosol particles from the sample flow to avoid possible evaporation of aerosol particles in the inlet of the PTR-MS (Tillmann et al., 2010). In the SAPHIR chamber a high resolution time of flight (HR-TOF) version of the PTR-MS (Jordan et al., 2009) was used in analogue to the AIDA measurement.

The aerosol chemical composition was characterised online using an aerosol mass spectrometer (HR-TOF-AMS, Aerodyne Research Inc.). The HR-TOF-AMS was connected to the chambers via stainless steel tubes (4 mm ID). The HR-TOF-AMS working principles and modes of operation are explained in detail elsewhere (Jayne et al., 2000; DeCarlo et al., 2006). Particles with vacuum aerodynamic diameters between 60 and 600 nm were focused by an aerodynamic lens, vaporised at about 600 K with subsequent electron impact ionisation (70 eV). The resulting fragment cations were recorded using a time of flight (TOF) mass spectrometer. Optional chopping of the particle beam and measurement of the particle time of flight before vaporisation allowed for size-resolved measurement of chemical composition. The relatively high fragmentation largely eliminated molecular specificity but provided accurate values for the total organic mass along with characteristic fragments indicating the oxidation extent with a time resolution of 10 min.

Particle number and size distribution measurements were used to determine absolute particle number and volume concentrations. At the AIDA chamber particle number concentrations were measured with three condensation particle counters (CPC 3022A, 3025A and CPC 3076A, TSI) outside the thermostated housing via stainless steel tubes extending 35 cm into the chamber. The absolute uncertainty of the number concentrations was estimated to ± 20 % by comparison of the different CPCs with each other and with an electrometer (3068, TSI). Size distributions were obtained using two mobility particle sizers (DMA 3071 and CPC 3010, TSI), one outside (SMPS) and one inside the thermostated housing (DMPS). Typical time intervals for size distribution measurements inside the thermostated housing were 25 min (DMPS) and outside 5 min (SMPS). Volume size distributions were normalised to the total number concentrations and integrated to obtain particle volume concentrations. The uncertainty of the particle volume concentrations obtained this way was estimated to be ± 30 % taking into account the uncertainty in the total number concentrations

and the relative importance of the larger particles. SOA mass concentrations were calculated from the measured volume concentrations using densities determined by Saathoff et al. (2009), i.e. $(1.25 \pm 0.10)\,\mathrm{g\,cm^{-3}}$ for α-pinene SOA and $(1.3 \pm 0.2)\,\mathrm{g\,cm^{-3}}$ for limonene SOA.

In the SAPHIR chamber the number size distribution was measured by a TSI SMPS3080 system equipped with a TSI UWCPC3786. The SMPS system was connected to the chamber by a 3 m long vertical and 50 cm long horizontal stainless steel line. The HR-TOF-AMS sampled from the same vertical line with a 130 cm horizontal line, which was pumped with a total flow of $380\,\mathrm{ml\,min^{-1}}$. The analysis of the particle data in SAPHIR was based on the combination of AMS and SMPS data. An effective density (ρ_{eff}) was calculated from the modal particle diameter of the volume size distribution measured with the SMPS and the modal particle diameter of the mass size distribution measured with the AMS (Bahreini et al., 2005) yielding an average ρ_{eff} of $1.3 \pm 0.1\,\mathrm{g\,cm^{-3}}$. This is in good agreement with values reported previously by Saathoff et al. (2009). The SMPS data were converted to particle mass by applying ρ_{eff}. In the evaluation of AMS data we applied a relative ionization efficiency of 1.4 (relative to ammonium nitrate) for the SOA. The organic mass observed by AMS was highly correlated with the SMPS derived mass ($R = 0.9997$); however, the absolute values were significantly lower by a factor of 0.38 ± 0.01. Herein only data with mass modal positions >85 nm were considered to ensure that all particles were well within the working window of the aerodynamic lens. The slope indicates a reduced AMS collection efficiency of about 40 % compared to NH_4NO_3 particles that were used for calibration of the ionisation efficiency. At the moment we cannot explain why this is the case, however, reduced collection efficiency has been observed before in lab and field studies (Matthew et al., 2008; Buchholz, 2010; Virtanen et al., 2010).

In the AIDA experiments, the concentration of selected aerosol constituents, i.e. pinonic, pinic and 3-methyl-1,2,3-butanetricarbocylic acid (MBTCA) were derived from on line APCI/MS and off- line LC-MS measurements. Pinic and pinonic acid are well known products from α-pinene oxidation and MBTCA has recently been confirmed to be a major α-pinene SOA constituent, probably formed from the OH-radical reaction of pinonic acid (Szmigielski et al., 2007). Details on the measurements and implications can be found elsewhere (Müller et al., 2011) and a just brief description is presented here. After passing a charcoal denuder to remove gas phase organics the particles were directly introduced into a modified Atmospheric-Pressure-Chemical-Ionisation (APCI) source of a commercial LC-Ion trap system (LCQ, Finnigan MAT, USA) (Hoffmann et al., 1998, 2002). The three targeted carboxylic acids form stable molecular ions in the negative ion mode and were measured with a very high temporal resolution (about 1 min) with the on-line APCI/MS. The identification of the compounds was realised by on-line MS/MS experiments and the comparison of the spectra with reference substances. The APCI parameters were set to: 2 µA discharge current, 623 K vaporiser temperature, 473 K capillary temperature, −7.8 V capillary voltage, 16.4 V lens voltage. The sheath gas flow rate was set to 5 units (arbitrary units defined by the instrument software). The APCI/MS/MS experiments were recorded at different collision energies and helium was used as collision gas. Nevertheless, the on-line technique provides no separation of the analytes before ionisation and detection. Therefore, these results can be affected by isobaric interferences and an unambiguous identification of single compounds is often difficult. Consequently, beside on-line APCI-MS also filter samples were taken and analysed later in the laboratory by extraction LC-MS (Reinnig et al., 2008). Both methods were applied to the same set of experiments (Müller et al., 2011).

2.2 Experimental procedures

A summary of the experiments with corresponding experimental conditions is found in Table 1. The initial SOA were produced from ozonolysis of (1S)-(-)-α-pinene (99 %, Aldrich) or (S)-(-)-limonene (>97 %, Merck) using 160–400 ppb ozone in excess. In the AIDA chamber the initial aerosol was produced at different temperatures (273, 293 and 313 K) with ozone in excess and the subsequent OH oxidation was performed using ozonolysis of tetramethyl-ethylene (TME) in the dark (Lambe et al., 2007). Before each experiment, the AIDA chamber was evacuated to typically 1 Pa total pressure, flushed two times with 10 hPa of synthetic air and filled to atmospheric pressure (∼1000 hPa) with humidified or dry synthetic air (low hydrocarbon grade, Basi). In most experiments ozone was first added to the chamber to measure any level of background particle formation before the terpene was added. These particles were generally formed 15–20 min after the addition of ozone in varying number concentrations but with negligible mass concentrations. Ozone was generated by a silent discharge generator (Semozon 030.2, Sorbios) in mixing ratios of about 3 % in pure oxygen and added to the chamber either directly or after dilution in a 1 l glass bulb with a flow of 5 SLM of synthetic air. Defined amounts of the terpenes were then added by evaporating 1–4 hPa into 1 and 2 l glass bulbs, diluting them with synthetic air, and flushing the contents into the chamber with 10 LPM synthetic air for 3 min. In the absence of seed particles this terpene-ozone mixture resulted in rapid particle nucleation with subsequent growth of the aerosol. The aerosol mass reached a plateau and was characterised in detail before addition of TME to initiate OH oxidation.

In order to produce desired amounts of OH radicals the ozone level was increased to 500–900 ppb and the TME was added continuously with $21–42\,\mathrm{ppb\,h^{-1}}$. The OH radical concentrations generated this way reached values between 1 and 0.2×10^7 molecules $\mathrm{cm^{-3}}$ for the α-pinene experiments

Table 1. Summary of experimental conditions. OH levels in AIDA were estimated by using the MCM 3.1 model. For SAPHIR the OH-levels were measured using LIF. The total SOA mass before OH production was initiated and ΔSOA mass produced during OH oxidation were estimated using density corrected SMPS data.

Experiment (Temperature/K) (RH/%)	Precursor concentration (ppb)	SOA mass ($\mu g\,m^{-3}$)	Addition of TME ($ppb\,h^{-1}$)	[OH] ($10^6\,cm^{-3}$)	ΔSOA mass ($\mu g\,m^{-3}$)	$VFR_{383\,K}$ [b]	ΔN_{VFR} [c]
AIDA, MUCHACHAS I							
SOA08-3[a] (273, 35)	α-pinene 14	31[d]	21–42	6–10	7[d] (23 %)	0.43	0.05
SOA08-1[a] (293, 42)	α-pinene 20	20[d]	23	3–4	11[d] (55 %)	0.53	0.06
SOA08-14 (293, 42)	α-pinene 33	43[d]	21	2.0–3.5	22[d] (51 %)	0.52	0.04
SOA08-6[a] (313, 20)	α-pinene 56	35[d]	24	∼2	6[d] (17 %)	0.60	>0.01
SOA08-13 (273, 36)	Limonene 10	42[d]	21	n.a.	3–7[d] (9–20 %)	0.53	0.01
SOA08-12 (293, 37)	Limonene 16	34[d]	23	n.a.	5[d] (25 %)	0.55	0.03
SOA08-11 (313, 21)	Limonene 16	21[d]	24	n.a.	15[d] (71 %)	0.69	0.03
SAPHIR, MUCHACHAS III							
SA10 (day 1) (296, 43)[f]	α-pinene 40	36[d]/60[e]	–	1.6& 5.1 (14[d]/9 %[e])	0.44	>0.01	
SA10 (day 2) (296, 18)[f]	–	6.7[d]/67[e]	–	2.4	2.6 (39[d]/4 %[e])	0.54	0.05
SA10 (day 3) (293, 10)[f]	–	1.5[d]/69[e]	–	2.0	1.0 (67[d]/1 %[e])	0.60	> 0.02

[a] Ammonium sulphate seed particle used. [b] VFR (383 K) at the start of the OH enhanced exposure. [c] VFR after one hour of OH exposure normalised to the starting point of the OH addition. [d] Not corrected for wall losses. [e] Corrected for wall losses. [f] Daytime average.

as estimated from MCM 3.1 simulations constrained to measured decay or formation rates of tracer compounds (3-pentanol, pinonaldehyde and acetone). The analysis of the 3-pentanol decay during TME ozonolysis suggests a very similar range of OH radical concentrations for the limonene experiments. The OH radical levels reached in the AIDA chamber depend inversely on temperature mainly due to lower concentrations of reactive volatile organic compounds at lower temperatures. Simulations of the α-pinene experiments were done with the aerosol behaviour code COSIMA (Naumann, 2003) supplemented with a recently developed SOA module (Saathoff et al., 2009). Here, the assumption of four proxies of different volatility proved sufficient to reproduce the experimentally determined time evolutions of mass and number concentrations and of the size distribution for α-pinene SOA.

The SAPHIR chamber experiments were designed to focus on the use of natural sunlight and long timescales. Experiments were conducted during three successive days, allowing for prolonged and repeated oxidation of the air mass. In the SAPHIR chamber the initial aerosol was produced in the dark from 40 ppb of α-pinene using ozone in 4-fold excess. When α-pinene dropped below 5 % of its initial value the chamber roof was opened and the reaction mixture in the chamber was exposed to natural sunlight. The photolysis of ozone in presence of water and a background HONO source (Rohrer et al., 2005) were producing OH radicals up to $3 \times 10^6\,cm^{-3}$ on the first day and up to $4 \times 10^6\,cm^{-3}$ on the following two days. The concentrations of the OH radicals were directly determined by LIF spectroscopy (Holland et al., 2003; Lu et al., 2011). The OH-concentration was up to an order of magnitude less than in the AIDA experiments. The OH radicals oxidised the residual α-pinene and the products of the previous ozonolysis.

There are two major differences between the AIDA and SAPHIR experiments: the method of OH generation and the nature and magnitude of particle and vapour losses. In AIDA OH was generated via dark ozonolysis, while in SAPHIR it was generated via solar ozone photolysis. SOA losses in AIDA are dominated by irreversible deposition of acidic vapours to the chamber walls with a time constant of $\sim(1.8–3.8)\times10^{-4}\,s^{-1}$ as determined from the COSIMA simulations also in experiments with pure acids in the AIDA chamber (Müller et al., 2011) and in agreement with previous studies (Saathoff et al., 2009). Particle deposition to the AIDA wall is modelled depending on particle size, the rate coefficient amounting to $1.1 \times 10^{-5}\,s^{-1}$ for 50 nm, $4.4 \times 10^{-6}\,s^{-1}$ for 100 nm, and to $1.9 \times 10^{-6}\,s^{-1}$ for 200 nm in diameter, respectively. Typical dilution rates in AIDA due to replaced sampling air were of order 5 % per day. The mixing fan, operated throughout all AIDA experiments, ensured homogeneous mixing within 1–2 min.

In the SAPHIR a permanent flow of synthetic air compensates for sample withdrawal, maintaining an over pressure of about 50 Pa. In the SA10 experiment this replenishment flow was on average $9\,m^3\,h^{-1}$. This results in an average

residence time of about 30 h, or a dilution loss rate coefficient of $9.35 \times 10^{-6}\,s^{-1}$ and compares well with the directly observed dilution rates of H_2O and CO_2 with loss coefficients of $9.1 \times 10^{-6}\,s^{-1}$ and $9.2 \times 10^{-6}\,s^{-1}$, respectively. The loss by dilution applies equally to suspended particles, vapours, and gases. Particles were subject to additional losses, which were determined step by step after correction for the dilution loss (lifetime/loss coefficient): wall deposition in the dark (37.5 h, or $7.41 \times 10^{-6}\,s^{-1}$), wall deposition during the day (11 h, $2.50 \times 10^{-5}\,s^{-1}$), and wall depositing while mixing with the ventilator fan (7 h, $4.0 \times 10^{-5}\,s^{-1}$). As a consequence the particle e-folding lifetimes (particle concentration equal to 1/e times the start concentration) in the chamber were (a) ca. 4 h, when the roof was open and the ventilator was switched on for mixing, (b) ca. 6 h 40 min, when the roof was open and the ventilator was switched off and (c) ca. 16 h 30 min, when the roof was closed. Because of the narrow size distribution (GSD = 1.3) size effects were neglected.

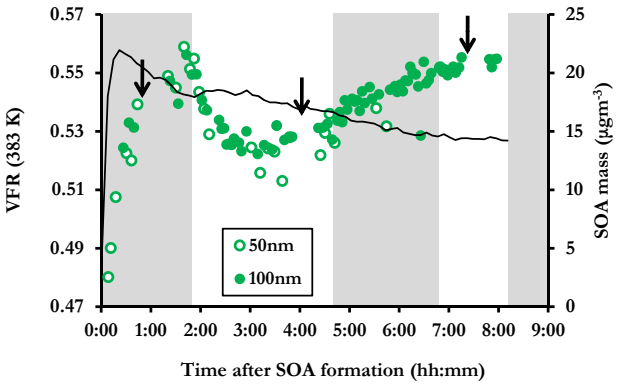

Fig. 1. The change in VFR (383 K) with time during experiment SOA08-12 (limonene) in AIDA, white areas indicate ageing with OH radicals (TME addition) and the black arrows when. thermograms were started. The black solid line is the SOA mass present in AIDA as measured with SMPS.

3 Results and discussion

3.1 Summary

A summary of the experimental results including VFR (383 K), observed SOA masses, and calculated OH levels is presented in Table 1. Clearly precursors, concentration levels, and temperature all have effect on the thermal properties of the aerosol. The VFR (383 K) for "fresh" α-pinene/O_3 SOA in this study ranges from 44 to 55 %, depending on the actual experimental conditions. The VFR (383 K) for α-pinene/O_3 SOA in earlier thermodenuder/VTDMA studies ranged from 20 to 50 %, e.g. An et al. (2007), Jonsson et al. (2007); Stanier et al. (2007), Cappa and Wilson (2011) and Tritscher et al. (2011). However the comparison of different evaporative systems should be taken with some care since the evaporation of SOA, thus obtained VFR, usually is measured in a non-equilibrium mode and will depend on the residence time and design of the heating unit (Riipinen et al., 2010). Keeping this in mind the observations of VFR (383 K) in Table 1 are comparable to the results from the previous studies.

In the following specific experiments are used for illustration, but the results are general unless indicate otherwise. Figure 1 shows the VFR (383 K) and uncorrected SOA mass for particles produced from ozonolysis of limonene at 293 K (SOA08-12). After addition of limonene (time = 0), SOA was formed quickly with the mass reaching a peak after about 0.5 h. The VFR (383 K) increased during this period and continued to increase even after the peak SOA mass was reached. This can be understood by a continuous loss of semi-volatile ozonolysis products to maintain equilibrium when aerosol mass decreased as will be discussed below. As soon as the OH radicals were generated, the VFR (383 K) begin to decrease as additional SOA mass was produced. This new material changed the composition of the particles, resulting in a more volatile aerosol. After some time of OH exposure the decrease in VFR (383 K) slowed down and eventually began to increase again. In a subsequent generation of OH radicals roughly 7 h after the initial SOA formation, neither additional SOA formation nor a decrease in VFR (383 K) was observed.

For the experiment shown in Fig. 1, the recording of thermograms began at the periods marked with arrows: just before addition of TME (the initiation of OH exposure), and towards the end of the two OH exposure periods. Figure 2 shows that there were only small differences between the two thermograms before and after the OH exposure period, even though the time trend in Fig. 1 clearly shows a significant effect of the TME addition. From the data presented in Fig. 2, one can conclude that at higher evaporative temperatures $T > 395$ K the aged aerosol (open circles) has higher VFR while at $T < 395$ K (closed circles) it is the opposite. In other words, the thermogram broadened somewhat after OH exposure. These observations can be explained by a long-term increase of low volatility compounds (>395 K) and a short-term increase of semi-volatile compounds (<395 K) due to OH radical reactions as discussed below.

3.2 Ozonolysis of precursor

The VFR dropped sharply and SOA mass increased whenever precursor gas was added to the chamber in the presence of pre-existing SOA. In the experiment shown in Fig. 3, limonene was added two times in the presence of pre-existing aerosol (indicated by arrows in the Fig.) and the VFR (383 K) promptly decreased when this new SOA mass was produced. The fresh SOA was evidently relatively volatile. After the SOA formation in the beginning of the experiment, the fresh SOA became progressively less volatile with time, resulting

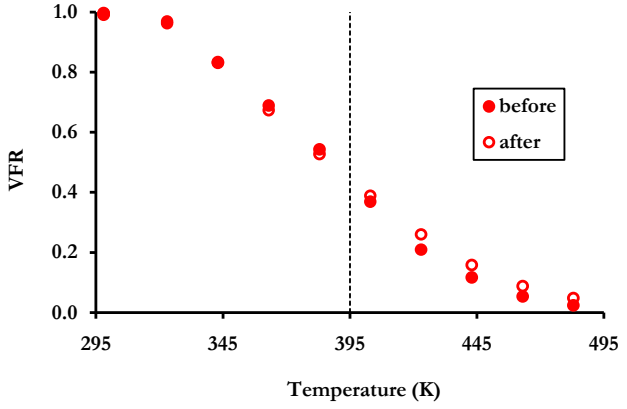

Fig. 2. The temperature dependence for the VFR, i.e. thermograms, before and after limonene SOA ageing in AIDA experiment SOA08-12. The dashed line indicates 395 K.

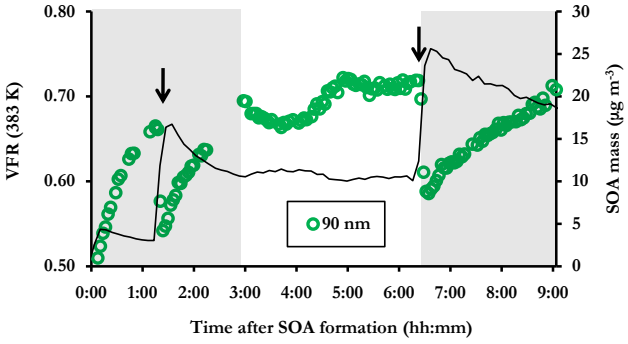

Fig. 3. VFR (383 K) of limonene SOA produced during SOA08-11 in the AIDA chamber and the change in measured SOA mass with time (black line). The white area indicates ageing with OH radicals (TME addition) and the black arrows show when limonene was added.

in an increase in VFR (383 K). The main explanation of this effect in the AIDA chamber is that acidic vapours were rapidly lost via uptake to the aluminium walls. Once the production of semi-volatile products (SVOC) stopped, the concentration of semi-volatile products in the gas phase decreased due to this uptake. To maintain equilibrium a net evaporation of SVOCs from the aerosol particles occurred, making them less volatile. A less pronounced effect on the VFR (383 K) is seen in the SAPHIR chamber (with FEP walls) where SOA losses are dominated by dilution and some deposition of particles on the walls and not primarily by the loss of gases. This is in contrast to AIDA and possibly teflon film chambers with smaller surface to volume ratios (Matsunaga et al., 2010). However, even simple dilution will shift the partitioning of semi-volatile compounds towards the gas phase, again reducing SOA volatility (Donahue et al., 2006). This decrease in volatility is then observed as an increase in VFR (383 K) with time. These observations confirm that the SOA is substantially semi-volatile under ambient conditions (Grieshop et al., 2007).

3.3 OH radical chemistry

When OH radicals were produced, gaseous SVOCs and IVOCs were oxidised and the partitioning equilibrium was shifted towards the condensed phase. This occurred using either the dark ozonolysis of TME in the AIDA chamber or using photochemistry by opening the roof in SAPHIR. As with the SOA initially produced in the ozonolysis of the precursor monoterpene, this new SOA changed the particle composition, making it more volatile than the pre-existing aerosol. This is shown as a decrease in VFR (383 K) promptly after the onset of the OH exposure. This behaviour is illustrated in Fig. 4 for α-pinene SOA; in this experiment TME addition started 2 h after the initial SOA formation, as indicated by the white area. Figure 4 also shows results of COSIMA simulations for the time evolution of the condensed phase concentrations of three condensable proxy compounds. COSIMA simulates four proxy products: a low-volatility product (pure component vapour pressure: 6.5×10^{-11} bar); a semi-volatile ozonolysis product (4.7×10^{-9} bar); a secondary semi-volatile product (3.0×10^{-10} bar); and a fourth product that does not partition into the particulate phase. The secondary semi-volatile proxy is mainly formed from the fourth proxy via OH oxidation but to a lesser extent also from the second proxy. In Fig. 4 the calculated total SOA masses for cases with and without OH radical production by TME ozonolysis are plotted. The low-volatility ozonolysis proxy decreases slowly during the entire experiment while the semi-volatile proxy decreases rapidly and is almost completely removed by vapour wall loss after four hours. This fast decrease can explain the rapid increase in VFR (383 K) observed during the first two hours of the experiment. The increase in aerosol mass after TME addition at 2 h is attributed to the formation of the OH product proxy. Some compounds represented by that proxy were also formed from the OH reaction of primary products produced during the initial ozonolysis (no OH scavenger was used in the experiment) but about $^3/_4$ of those compounds were formed after the OH source was switched on. This dramatic change in particle composition was observed as a large decrease in VFR (383 K) by 15 %. The precursors (proxy 4) were then consumed and the trend in VFR (383 K) changed and increased again as semi-volatile constituents continued to be lost to the chamber walls.

The effects of natural oxidant levels generated by natural actinic fluxes were investigated in the SAPHIR chamber. Figure 5 shows the time evolution of the particle mass determined by AMS before and after wall loss corrections together with the (VFR 383 K) determined by the VT-DMA. The experimental conditions for the ozonolysis in experiment SA10 were comparable to experiment SOA08-14,

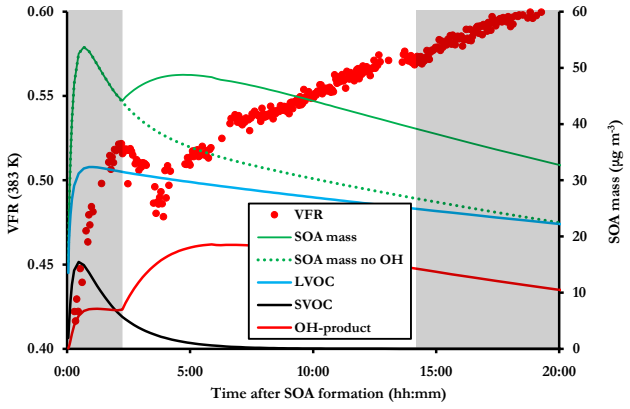

Fig. 4. Comparison of VFR (383 K) measured during SOA08-14 (α-pinene + ozone, with OH ageing) and the calculated SOA mass based on a SOA model using 4 products of different volatility, modelled SOA mass without additional OH chemistry. Low volatile (LVOC), semi-volatile (SVOC) and OH-product. The white area indicates ageing with OH-radicals (TME addition).

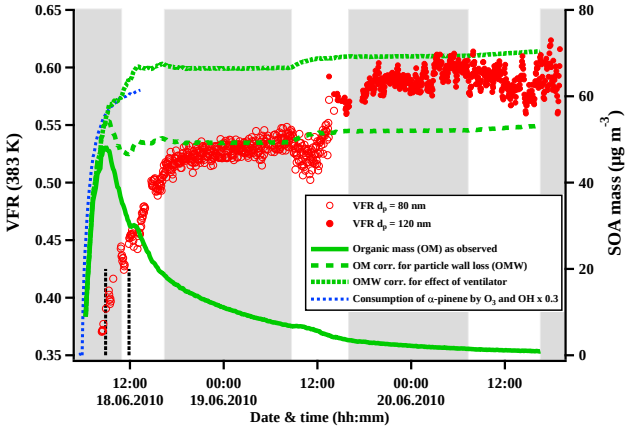

Fig. 5. VFR (383 K) of 80 nm and 120 nm particles for α-pinene SOA produced in SAPHIR (SA10). The change in SOA mass with time before (green line) and after loss corrections without (green dashed line) and with ventilator on (green dotted line). The ventilator was switched on in the time interval between the black dashed lines. The white areas indicate when the roof was open and the reaction mixture was exposed to sunlight. The blue dotted line shows the turnover of α-pinene due to reaction with O_3 and OH, which was multiplied by 0.3 in order to estimate the contribution of α-pinene oxidation, compared to the oxidation of ozonolysis products.

though the loss terms associated with each experiment were quite different. A simplified mass balance for the total SOA during the SA10 experiment is shown in Fig. 5. This accounts or different particle wall loss rates during different periods, as described above, as well as losses from ventilation. After correcting for particle wall losses, there are clearly visible upward steps in the SOA mass during each OH ageing episode. During the first day some of the fresh SOA is attributable to the oxidation of residual α-pinene by O_3 and OH after the chamber roof was open. From the turnover by α-pinene in this period we estimate this to be about 2 µg m^{-3}. The rest of the increases in SOA mass provide a lower limit of mass gain of the particles under exposure to sunlight/OH. The extra gain by reaction of the oxidised vapours by OH was 5.1 µg m^{-3} on the first day, 2.4 µg m^{-3} on the second day, and 1.0 µg m^{-3} on the third day in the presence of about 36 µg m^{-3}, 7 µg m^{-3}, and 1.5 µg m^{-3} SOA, respectively (Table 1). Since determining the total formation of new condensable SOA mass upon ageing, however, requires consideration of the effects of dilution as well as condensation of vapours to particles deposited on the chamber wall, the exact mass balance SOA including ageing effects in SAPHIR (as with all chamber experiments) remain uncertain, unless the vapour loss rates are known. For these reasons the actual extra SOA mass is likely significantly greater than the steps in total mass in Fig. 5. However, the mass balances for all MUCHACHAS experiments (including these) can be described with a common model, which will be reported elsewhere (Donahue et al., 2011). The major concern of this work is the effect of OH oxidation on particle volatility. The patterns in VFR (383 K) for SA10 shown in Fig. 5 and SOA08-14 shown in Fig. 4 are similar, with dips in VFR (383 K) during OH ageing periods superimposed on a steady increase in VFR over the entire experiment. The dips during OH ageing are somewhat smaller (≈10 %) in the SAPHIR, but the vapour loss mechanisms and OH levels are different. In AIDA, acid vapours are lost to the chamber walls but otherwise there is minimal dilution, while in SAPHIR, vapours and particles are lost due to dilution from the chamber make-up flow. In addition, the OH levels (Table 1) in SOA08-14 were roughly twice as large as in SA10, leading to an accentuated signal at the onset of ageing. During the second and third days in SAPHIR, after very substantial dilution, there are still clearly evident dips in VFR (383 K) upon OH exposure, indicating that residual vapours remained to contribute to an additional (relatively volatile) second-generation SOA.

3.4 Temperature effect during ozonolysis

Figure 6 shows the thermograms for experiments at 273, 293 and 315 K collected after the initial aerosol has been produced, i.e. 1–1.5 h after the addition of the precursor. Clearly the SOA formed from the ozonolysis of α-pinene shows a more volatile behaviour with lower experimental temperature, which is in line with the results reported by Jonsson et al. (2007). This volatility difference is most pronounced between 293 and 313 K with less difference between 273 and 293 K. It should be stressed that in the VTDMA set-up the sampled aerosol was pre-conditioned to room temperature before entering the VTDMA. Specifically, the sample passed through a copper tube, held at ambient temperature, with a residence time of one minute. This ensured that the volatility

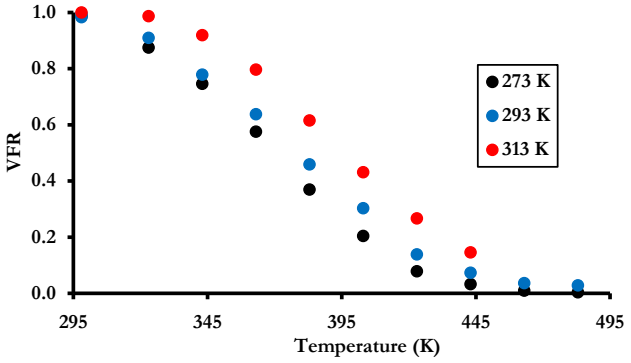

Fig. 6. The temperature dependence of VFR for α-pinene SOA from ozonolysis reactions at 273 K, SOA08-3, 293 K, SOA08-1 and 313 K, SOA08-6 in the AIDA chamber before OH induced ageing.

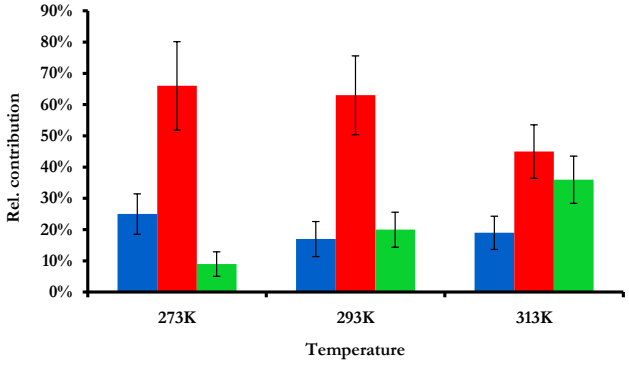

Fig. 7. Chemical composition of the organic aerosol at 1–1.5 h after the addition of the precursor. Relative contribution compared to the total amount of three selected acidic oxidation products, of α-pinene at different temperatures, pinonic acid (blue bars), pinic acid (red bars) and MBTCA (green bars). Error bars were calculated from the relative standard deviation of the averaged measurement time.

measurements represented the aerosol thermal characteristics at a standard temperature, independent of the reaction chamber temperature. The observed differences in volatility for the three aerosols were therefore assumed to be induced by changes in chemical composition rather than an effect of temperature induced changes in the gas to particle partitioning.

For the three α-pinene experiments shown in Fig. 6 the aerosol composition was measured using APCI-MS analysis. Figure 7 compares the chemical characterisation of the organic aerosol by APCI-MS performed 1–1.5 h after the addition of α-pinene at the three different temperatures (273, 293, and 313 K). Figure 7 shows the relative contribution of three prominent α-pinene SOA products: pinonic acid (a ketomonocarboxylic acid), pinic acid (a diacid), and 3-methyl-1,2,3-butanetricarboxylic acid (MBTCA, a triacid) (individual structures are shown in Fig. 8a–c). The most obvious feature shown in Fig. 7 is the increasing relative fraction of MBTCA at higher temperatures in the reaction vessel. The larger relative contribution of the compound with the lowest volatility is consistent with the volatility measurements shown in Fig. 6. More details on these products, the speciation in the AIDA experiments and its chemistry is found in the paper by Müller et al. (2011).

3.5 Temperature effect of OH ageing

Temperature also influenced the OH ageing period of the experiments. For the Limonene system a larger increase in SOA mass was observed at higher temperatures due to OH ageing (Table 2). Furthermore, the decrease in VFR (383 K) of the resulting SOA after exposed to OH radicals was more pronounced in the high-temperature experiments (Fig. 9). This is consistent with expectations since the SVOCs and even the IVOCs formed in the ozonolysis are preferentially transferred into the condensed phase at lower temperatures and thus not available for gas-phase OH-radical reactions.

A similar pattern was observed in the α-pinene experiments at 273 K and 293 K. However, for the experiment done at 313 K the OH ageing effect on VFR (383 K) was absent while a mass increase was observed. The mass increase was less than for 283 and 293 K but still significant. The initial VFR (383 K), before the OH ageing phase, was here 0.60 compared to 0.43 and 0.52–0.53 for 273 and 293 K, respectively. One complicating factor is that in all except one of the α-pinene experiments ammonium sulphate seed aerosols were used. The seed aerosol complicated the analysis of VFR responses, even though most of the 100 nm particles selected by the first DMA contained significant fractions of SOA. The 313 K α-pinene experiment also had significantly lower OH radical concentrations than the 273 and 293 K experiments. Consequently, there was less potential for ageing thus causing no observed changes in volatility and a modest relative mass change.

3.6 Partitioning

The volatility of the SOA provides a consistent framework to understand the observed behaviour, both before and after ageing by OH radicals. The "fresh" SOA clearly contains semi-volatile constituents, which as vapours can be preferentially lost to reactive walls such as those in the AIDA chamber (Saathoff et al., 2009). Partitioning effects likely also influence the SAPHIR experiments, with evaporation driven by the dilution associated with gas replenishment. However, the loss mechanisms in the two chambers are quite different, with preferential loss of (some) vapours in AIDA in contrast to balanced particle and vapour losses from dilution in SAPHIR. The onset of OH chemistry occurs at a point in the experiments where the existing particles have been pre-aged by partitioning (i.e. net evaporation) driven primarily

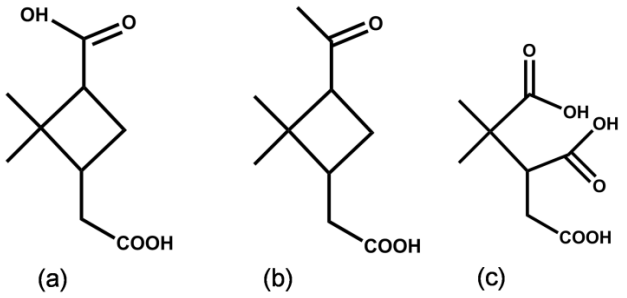

Fig. 8. Chemical structures of pinonic acid **(a)** pinic acid **(b)** and 3-methyl-1,2,3-butanetricarboxylic acid (MBTCA) **(c)**.

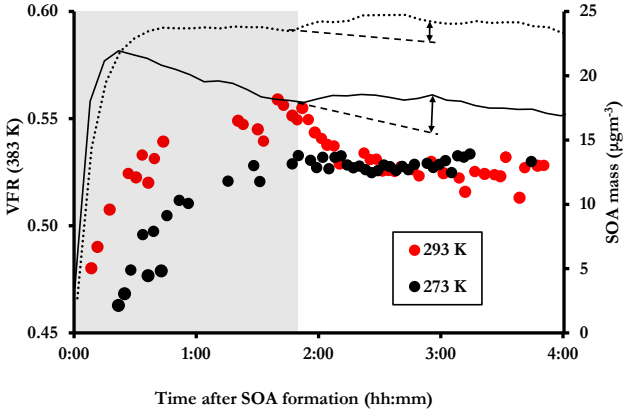

Fig. 9. Comparison of VFR (383 K) for limonene SOA produced at 293 K, SOA08-12 and 273 K, SOA08-13. The white area indicates OH ageing. The uncorrected SOA mass 293 K (solid line) and 273 K (dotted line). The black arrows indicate SOA mass produced from OH ageing in AIDA.

by dilution and vapour losses to the walls. The resulting OH chemistry thus produces a new set of compounds that replenish the most volatile fraction of the SOA (increase in mass and decrease in VFR (383 K). The dominant effect on VFR (383 K) from OH chemistry is thus attributed to a gas phase process interacting via partitioning with the condensed phase.

Direct measurement of key SOA constituents supports the bulk measurements of SOA mass and volatility. Specifically, the time-dependent trace for the semi-volatile model product in Fig. 4 is consistent with APCI-MS observations of semi-volatile acids such as cis-pinonic acid that tend to decay due to wall losses. Less volatile acids, such as pinic acid and especially MBTCA, show much less decay because only a very small fraction exists in the vapour phase in equilibrium. Consequently, the overall loss rate of these compounds (in both condensed and vapour phases) from vapour deposition to the chamber walls is slow. While the behaviour of the semi-volatile acids is consistent with ageing reactions converting the semi-volatile species to much less volatile products, the overall broadening of the thermograms (i.e. Fig. 2) confirms that in addition to this ageing of first-generation semi-volatile products, additional semi-volatile SOA is produced during the ageing reactions from more volatile first-generation products (i.e. pinonaldehyde, etc). The decrease in VFR(383 K) is attributed to gas phase chemistry driven by partitioning while the increase of VFR (>395 K) could partly be an effect of condensed phase chemistry that via partitioning leads to a mass increase, see e.g. Kalberer et al. (2004) and the review by Hallquist et al. (2009). Recently, the heterogeneous reaction of organics with OH has been explored in several studies see e.g. McNeill et al. (2008) and Lambe et al. (2009). In the study of McNeill et al. (2008) the surface reaction was followed by a volatilisation in line with a decrease in VFR (383 K). However, this is contradictory to the observed mass increase in all of the present experiments (Table 1).

4 Conclusions

In a series of experiments within the MUCHACHAS campaign, volatility was used as a signature for changes in composition of SOA (ageing). Generally, the observed changes in volatility during the experiments can be explained by three processes: (1) initial oxidation of the parent terpenes and subsequent production of fresh SOA material, (2) oxidation by OH radicals of gas phase products to produce compounds partitioning to the particle phase and (3) the effect of the actual design of the chambers and the experiments where walls and dilution contribute to changes in absolute gas and particle phase concentrations. The effects of OH chemistry (the main focus of this work) are influenced by the availability of compounds in the gas-phase. Consequently, the effect of OH chemistry was observed to be less pronounced in high concentration and low temperature experiments when lower relative amounts of semi-volatile material were available in the gas phase. This oxidation of gaseous SVOCs by OH radicals or oxidation of the unsaturated precursors by ozone caused a short-term ageing effect giving more volatile SOA. This effect is consistent with observations from the MUCHACHAS experiments at the PSI chamber by Tritscher et al. (2011). This short-term ageing was observed on top of a long term evolution in VFR (383 K) caused by transport of SVOCs to the chamber walls or reduction of the aerosol mass by dilution, both of which resulted in a less volatile SOA. The results in the SAPHIR chamber show that these ageing processes will also occur during photo-chemical ageing. The effects depend on the amount of OH radicals and are thus smaller in magnitude in SAPHIR than in AIDA, where OH levels were higher.

The results of the experiments done at different temperatures clearly point out the behaviour of SOA compounds

with different volatilities. According to the temperature dependence of the partitioning coefficient, semi-volatile compounds such as pinic acid are mainly present in the particle phase at lower temperatures but in the gas phase at high temperatures. For more volatile compounds the partitioning is shifted towards the gas-phase fraction, as can be seen for pinonic acid. Finally, low volatile compounds are predominantly in the particle phase over the whole temperature range. The effect of OH chemistry thus decreases with decreasing temperatures but is still present in the low temperature experiments. This is also in accordance with a recent low temperature flow reactor study by Jonsson et al. (2008).

In order for pronounced OH ageing to occur the SVOC or IVOC must be found in the gas phase, i.e. the ageing is due to OH oxidation in the gas phase. Under the experimental conditions employed here there was no evidence that the aerosols themselves were oxidised by bulk or surface reactions, indicating that these heterogeneous processes are substantially slower than the homogeneous gas-phase ageing. In these experiments no definite proof for fragmentation or volatilisation of the SOA was found. However, it was demonstrated that using data from these two chambers, with their different characteristics, provided a consistent framework for understanding SOA volatility and the effect of OH radical ageing. In the atmosphere the OH ageing processes will depend on availability of products in the gas phase and the OH concentration. It will thus depend on many ambient properties, including temperature, actinic flux and the total amount of organic aerosol.

Acknowledgements. We thank the AIDA team at KIT and the SAPHIR team at FZJ for their effective support during the measurement campaigns. Eva Emanuelsson at University of Gothenburg is acknowledged for running the VTDMA in the SAPHIR experiments. The MUCHACHAS campaigns were supported by EUROCHAMP-2 (Integration of European Simulation Chambers for Investigating Atmospheric Processes) a research project within the EC 7th framework programmes. M. H. and K. S. in addition acknowledge support by Formas under contract 214-2006-1204, The Swedish Research Council under contract 80475101 and the Nanoparticles in Interactive Environments platform at the Faculty of Science at the University of Gothenburg.

Edited by: F. Keutsch

References

An, W. J., Pathak, R. K., Lee, B.-H., and Pandis, S. N.: Aerosol volatility measurement using an improved thermodenuder: Application to secondary organic aerosol, J. Aerosol Sci., 38, 305–314, 2007.

Andreae, M. O.: A New Look at Aging Aerosols, Science, 326, 1493–1494, doi:10.1126/science.1183158, 2009.

Bahreini, R., Keywood, M. D., Ng, N. L., Varutbangkul, V., Gao, S., Flagan, R. C., Seinfeld, J. H., Worsnop, D. R., and Jimenez, J. L.: Measurements of Secondary Organic Aerosol from Oxidation of Cycloalkenes, Terpenes, and m-Xylene Using an Aerodyne Aerosol Mass Spectrometer, Environ. Sci. Technol., 39, 5674–5688, doi:10.1021/es048061a, 2005.

Buchholz, A.: Secondary Organic Aerosols: Chemical Aging, Hygroscopicity, and Cloud Droplet Activation, Mathematisch-Naturwissenschaftliche Fakultät, Universität zu Köln, Köln, 128 pp., 2010.

Cappa, C. D. and Wilson, K. R.: Evolution of organic aerosol mass spectra upon heating: implications for OA phase and partitioning behavior, Atmos. Chem. Phys., 11, 1895–1911, doi:10.5194/acp-11-1895-2011, 2011.

D'Anna, B., Jammoul, A., George, C., Stemmler, K., Fahrni, S., Ammann, M., and Wisthaler, A.: Light-induced ozone depletion by humic acid films and submicron aerosol particles, J. Geophys. Res., 114, D12301, doi:10.1029/2008jd011237, 2009.

DeCarlo, P. F., Kimmel, J. R., Trimborn, A., Northway, M. J., Jayne, J. T., Aiken, A. C., Gonin, M., Fuhrer, K., Horvath, T., Docherty, K. S., Worsnop, D. R., and Jimenez, J. L.: Field-Deployable, High-Resolution, Time-of-Flight Aerosol Mass Spectrometer, Anal. Chem., 78, 8281–8289, doi:10.1021/ac061249n, 2006.

Donahue, N. M., Robinson, A. L., and Pandis, S. N.: Atmospheric organic particulate matter: From smoke to secondary organic aerosol, Atmos. Environ., 43, 94–106, doi:10.1016/j.atmosenv.2008.09.055, 2009.

Donahue, N. M., Henry, K. M., Mentel, T. F., Saathoff, H., Hoffmann, T., Salo, K., Tritscher, T., Barmet, P. B., Hallquist, M., DeCarlo, P. F., Dommen, J., Prevot, A. S. H., and Baltensperger, U.: Aging of Secondary Organic Aerosol: Connecting Chambers to the Atmosphere, Proc. Natl. Acad. Sci. USA, under review, 2011.

George, I. J. and Abbatt, J. P. D.: Heterogeneous oxidation of atmospheric aerosol particles by gas-phase radicals, Nat. Chem., 2, 713–722, 2010.

Grieshop, A. P., Donahue, N. M., and Robinson, A. L.: Is the gas-particle partitioning in alpha-pinene secondary organic aerosol reversible?, Geophys. Res. Lett., 34, L14810, doi:10.1029/2007gl029987, 2007.

Hallquist, M., Wenger, J. C., Baltensperger, U., Rudich, Y., Simpson, D., Claeys, M., Dommen, J., Donahue, N. M., George, C., Goldstein, A. H., Hamilton, J. F., Herrmann, H., Hoffmann, T., Iinuma, Y., Jang, M., Jenkin, M. E., Jimenez, J. L., Kiendler-Scharr, A., Maenhaut, W., McFiggans, G., Mentel, T. F., Monod, A., Prévôt, A. S. H., Seinfeld, J. H., Surratt, J. D., Szmigielski, R., and Wildt, J.: The formation, properties and impact of secondary organic aerosol: current and emerging issues, Atmos. Chem. Phys., 9, 5155–5236, doi:10.5194/acp-9-5155-2009, 2009.

Hoffmann, T., Bandur, R., Marggraf, U., and Linscheid, M.: Molecular composition of organic aerosols formed in the alpha-pinene/O-3 reaction: Implications for new particle formation processes, J. Geophys. Res.-Atmos., 103, 25569–25578, 1998.

Hoffmann, T., Bandur, R., Hoffmann, S., and Warscheid, B.: On-line characterization of gaseous and particulate organic analytes using atmospheric pressure chemical ionization mass spectrometry, Spectrochim. Acta, Part B, 57, 1635–1647, doi:10.1016/s0584-8547(02)00111-8, 2002.

Holland, F., Hofzumahaus, A., Schäfer, J., Kraus, A., and Pätz, H.-W.: Measurements of OH and HO_2 radical concentrations and photolysis frequencies during BERLIOZ, J. Geophys. Res., 108,

8246, doi:10.1029/2001jd001393, 2003.

Jayne, J. T., Leard, D. C., Zhang, X. F., Davidovits, P., Smith, K. A., Kolb, C. E., and Worsnop, D. R.: Development of an aerosol mass spectrometer for size and composition analysis of submicron particles, Aerosol Sci. Technol., 33, 49–70, 2000.

Jimenez, J. L., Canagaratna, M. R., Donahue, N. M., Prevot, A. S. H., Zhang, Q., Kroll, J. H., DeCarlo, P. F., Allan, J. D., Coe, H., Ng, N. L., Aiken, A. C., Docherty, K. S., Ulbrich, I. M., Grieshop, A. P., Robinson, A. L., Duplissy, J., Smith, J. D., Wilson, K. R., Lanz, V. A., Hueglin, C., Sun, Y. L., Tian, J., Laaksonen, A., Raatikainen, T., Rautiainen, J., Vaattovaara, P., Ehn, M., Kulmala, M., Tomlinson, J. M., Collins, D. R., Cubison, M. J., Dunlea, E. J., Huffman, J. A., Onasch, T. B., Alfarra, M. R., Williams, P. I., Bower, K., Kondo, Y., Schneider, J., Drewnick, F., Borrmann, S., Weimer, S., Demerjian, K., Salcedo, D., Cottrell, L., Griffin, R., Takami, A., Miyoshi, T., Hatakeyama, S., Shimono, A., Sun, J. Y., Zhang, Y. M., Dzepina, K., Kimmel, J. R., Sueper, D., Jayne, J. T., Herndon, S. C., Trimborn, A. M., Williams, L. R., Wood, E. C., Middlebrook, A. M., Kolb, C. E., Baltensperger, U., and Worsnop, D. R.: Evolution of Organic Aerosols in the Atmosphere, Science, 326, 1525–1529, doi:10.1126/science.1180353, 2009.

Johnson, D. and Marston, G.: The gas-phase ozonolysis of unsaturated volatile organic compounds in the troposphere, Chem. Soc. Rev., 37, 699–716, doi:10.1039/b704260b, 2008.

Jonsson, Å. M., Hallquist, M., and Ljungström, E.: Impact of Humidity on the Ozone Initiated Oxidation of Limonene, Δ3-Carene, and α-Pinene, Environ. Sci. Technol., 40, 188–194, 2006.

Jonsson, Å. M., Hallquist, M., and Saathoff, H.: Volatility of secondary organic aerosols from the ozone initiated oxidation of α-pinene and limonene, J. Aerosol Sci., 38, 843–852, 2007.

Jonsson, Å. M., Hallquist, M., and Ljungström, E.: The effect of temperature and water on secondary organic aerosol formation from ozonolysis of limonene, Δ3-carene and α-pinene, Atmos. Chem. Phys., 8, 6541–6549, doi:10.5194/acp-8-6541-2008, 2008.

Jordan, C., Fitz, E., Hagan, T., Sive, B., Frinak, E., Haase, K., Cottrell, L., Buckley, S., and Talbot, R.: Long-term study of VOCs measured with PTR-MS at a rural site in New Hampshire with urban influences, Atmos. Chem. Phys., 9, 4677–4697, doi:10.5194/acp-9-4677-2009, 2009.

Kalberer, M., Paulsen, D., Sax, M., Steinbacher, M., Dommen, J., Prevot, A. S. H., Fisseha, R., Weingartner, E., Frankevich, V., Zenobi, R., and Baltensperger, U.: Identification of polymers as major components of atmospheric organic aerosols, Science, 303, 1659–1662, 2004.

Kroll, J. H. and Seinfeld, J. H.: Chemistry of secondary organic aerosol: Formation and evolution of low-volatility organics in the atmosphere, Atmos. Environ., 42, 3593–3624, 2008.

Kroll, J. H., Donahue, N. M., Jimenez, J. L., Kessler, S. H., Canagaratna, M. R., Wilson, K. R., Altieri, K. E., Mazzoleni, L. R., Wozniak, A. S., Bluhm, H., Mysak, E. R., Smith, J. D., Kolb, C. E., and Worsnop, D. R.: Carbon oxidation state as a metric for describing the chemistry of atmospheric organic aerosol, Nat. Chem., online publication, available at: http://www.nature.com/nchem/journal/vaop/ncurrent/abs/nchem.948.html#supplementary-information, 2011.

Lambe, A. T., Zhang, J., Sage, A. M., and Donahue, N. M.: Controlled OH Radical Production via Ozone-Alkene Reactions for Use in Aerosol Aging Studies, Environ. Sci. Tecnol., 41, 2357–2363, doi:10.1021/es061878e, 2007.

Lambe, A. T., Miracolo, M. A., Hennigan, C. J., Robinson, A. L., and Donahue, N. M.: Effective Rate Constants and Uptake Coefficients for the Reactions of Organic Molecular Markers (n-Alkanes, Hopanes, and Steranes) in Motor Oil and Diesel Primary Organic Aerosols with Hydroxyl Radicals, Environ. Sci. Tecnol., 43, 8794–8800, doi:10.1021/es901745h, 2009.

Lindinger, W., Hansel, A., and Jordan, A.: On-line monitoring of volatile organic compounds at pptv levels by means of proton-transfer-reaction mass spectrometry (PTR-MS) medical applications, food control and environmental research, Int. J. Mass Spectrom. Ion Proc., 173, 191–241, doi:10.1016/s0168-1176(97)00281-4, 1998.

Lu, K. D., Rohrer, F., Holland, F., Fuchs, H., Bohn, B., Brauers, T., Chang, C. C., Häseler, R., Hu, M., Kita, K., Kondo, Y., Li, X., Lou, S. R., Nehr, S., Shao, M., Zeng, L. M., Wahner, A., Zhang, Y. H., and Hofzumahaus, A.: Observation and modelling of OH and HO_2 concentrations in the Pearl River Delta 2006: a missing OH source in a VOC rich atmosphere, Atmos. Chem. Phys. Discuss., 11, 11311–11378, doi:10.5194/acpd-11-11311-2011, 2011.

Matsunaga, A. and Ziemann, P. J.: Gas-Wall Partitioning of Organic Compounds in a Teflon Film Chamber and Potential Effects on Reaction Product and Aerosol Yield Measurements, Aerosol Sci. Technol., 44, 881–892, 2010.

Matthew, B. M., Middlebrook, A. M., and Onasch, T. B.: Collection Efficiencies in an Aerodyne Aerosol Mass Spectrometer as a Function of Particle Phase for Laboratory Generated Aerosols, Aerosol Sci. Technol., 42, 884–898, 2008.

McNeill, V. F., Yatavelli, R. L. N., Thornton, J. A., Stipe, C. B., and Landgrebe, O.: Heterogeneous OH oxidation of palmitic acid in single component and internally mixed aerosol particles: vaporization and the role of particle phase, Atmos. Chem. Phys., 8, 5465–5476, doi:10.5194/acp-8-5465-2008, 2008.

Müller, L., Reinnig, M. C., Naumann, K. H., Saathoff, H., Mentel, T. F., Donahue, N. M., and Hoffmann, T.: Formation of 3-methyl-1,2,3-butanetricarboxylic acid via gas phase oxidation of pinonic acid – a mass spectrometric study of SOA aging, Atmos. Chem. Phys. Discuss., 11, 19443–19476, doi:10.5194/acpd-11-19443-2011, 2011.

Naumann, K.-H.: COSIMA – a computer program simulating the dynamics of fractal aerosols, J. Aerosol Sci., 34, 1371–1397, doi:10.1016/s0021-8502(03)00367-7, 2003.

Ng, N. L., Canagaratna, M. R., Zhang, Q., Jimenez, J. L., Tian, J., Ulbrich, I. M., Kroll, J. H., Docherty, K. S., Chhabra, P. S., Bahreini, R., Murphy, S. M., Seinfeld, J. H., Hildebrandt, L., Donahue, N. M., DeCarlo, P. F., Lanz, V. A., Prévôt, A. S. H., Dinar, E., Rudich, Y., and Worsnop, D. R.: Organic aerosol components observed in Northern Hemispheric datasets from Aerosol Mass Spectrometry, Atmos. Chem. Phys., 10, 4625–4641, doi:10.5194/acp-10-4625-2010, 2010.

Pankow, J. F.: An absorption model of gas/particle partitioning of organic compounds in the atmosphere, Atmos. Environ., 28, 185–188, 1994.

Presto, A. A. and Donahue, N. M.: Investigation of α-Pinene + Ozone Secondary Organic Aerosol Formation at Low Total Aerosol Mass, Environ. Sci. Tecnol., 40, 3536–3543,

doi:10.1021/es052203z, 2006.

Rader, D. J. and McMurry, P. H.: Application of the tandem differential mobility analyzer to studies of droplet growth or evaporation, J. Aerosol Sci., 17, 771–787, doi:10.1016/0021-8502(86)90031-5, 1986.

Reinnig, M.-C., Müller, L., Warnke, J., and Hoffmann, T.: Characterization of selected organic compound classes in secondary organic aerosol from biogenic VOCs by HPLC/MS, Anal. Bioanal. Chem., 391, 171–182, doi:10.1007/s00216-008-1964-5, 2008.

Riipinen, I., Pierce, J. R., Donahue, N. M., and Pandis, S. N.: Equilibration time scales of organic aerosol inside thermodenuders: Evaporation kinetics versus thermodynamics, Atmos. Environ., 44, 597–607, doi:10.1016/j.atmosenv.2009.11.022, 2010.

Rohrer, F., Bohn, B., Brauers, T., Brüning, D., Johnen, F.-J., Wahner, A., and Kleffmann, J.: Characterisation of the photolytic HONO-source in the atmosphere simulation chamber SAPHIR, Atmos. Chem. Phys., 5, 2189–2201, doi:10.5194/acp-5-2189-2005, 2005.

Rollins, A. W., Kiendler-Scharr, A., Fry, J. L., Brauers, T., Brown, S. S., Dorn, H. P., Dubé, W. P., Fuchs, H., Mensah, A., Mentel, T. F., Rohrer, F., Tillmann, R., Wegener, R., Wooldridge, P. J., and Cohen, R. C.: Isoprene oxidation by nitrate radical: alkyl nitrate and secondary organic aerosol yields, Atmos. Chem. Phys., 9, 6685–6703, doi:10.5194/acp-9-6685-2009, 2009.

Saathoff, H., Möhler, O., Schurath, U., Kamm, S., Dippel, B., and Mihelcic, D.: The AIDA soot aerosol characterisation campaign 1999, J. Aerosol Sci., 34, 1277–1296, doi:10.1016/s0021-8502(03)00363-x, 2003.

Saathoff, H., Naumann, K.-H., Möhler, O., Jonsson, Å. M., Hallquist, M., Kiendler-Scharr, A., Mentel, Th. F., Tillmann, R., and Schurath, U.: Temperature dependence of yields of secondary organic aerosols from the ozonolysis of α-pinene and limonene, Atmos. Chem. Phys., 9, 1551–1577, doi:10.5194/acp-9-1551-2009, 2009.

Salo, K., Jonsson, Å. M., Andersson, P. U., and Hallquist, M.: Aerosol Volatility and Enthalpy of Sublimation of Carboxylic Acids, J. Phys. Chem. A, 114, 4586–4594, doi:10.1021/jp910105h, 2010.

Schlosser, E., Brauers, T., Dorn, H. P., Fuchs, H., Häseler, R., Hofzumahaus, A., Holland, F., Wahner, A., Kanaya, Y., Kajii, Y., Miyamoto, K., Nishida, S., Watanabe, K., Yoshino, A., Kubistin, D., Martinez, M., Rudolf, M., Harder, H., Berresheim, H., Elste, T., Plass-Dülmer, C., Stange, G., and Schurath, U.: Technical Note: Formal blind intercomparison of OH measurements: results from the international campaign HOxComp, Atmos. Chem. Phys., 9, 7923–7948, doi:10.5194/acp-9-7923-2009, 2009.

Stanier, C. O., Pathak, R. K., and Pandis, S. N.: Measurements of the Volatility of Aerosols from α-Pinene Ozonolysis, Environ. Sci. Tecnol., 41, 2756–2763, doi:10.1021/es0519280, 2007.

Szmigielski, R., Surratt, J. D., Gómez-González, Y., Van der Veken, P., Kourtchev, I., Vermeylen, R., Blockhuys, F., Jaoui, M., Kleindienst, T. E., Lewandowski, M., Offenberg, J. H., Edney, E. O., Seinfeld, J. H., Maenhaut, W., and Claeys, M.: 3-methyl-1,2,3-butanetricarboxylic acid: An atmospheric tracer for terpene secondary organic aerosol, Geophys. Res. Lett., 34, L24811, doi:10.1029/2007gl031338, 2007.

Tillmann, R., Hallquist, M., Jonsson, A. M., Kiendler-Scharr, A., Saathoff, H., Iinuma, Y., and Mentel, T. F.: Influence of relative humidity and temperature on the production of pinonaldehyde and OH radicals from the ozonolysis of alpha-pinene, Atmos. Chem. Phys., 10, 7057–7072, doi:10.5194/acp-10-7057-2010, 2010.

Tritscher, T., Dommen, J., DeCarlo, P. F., Barmet, P. B., Praplan, A. P., Weingartner, E., Gysel, M., Prévôt, A. S. H., Riipinen, I., Donahue, N. M., and Baltensperger, U.: Volatility and hygroscopicity of aging secondary organic aerosol in a smog chamber, Atmos. Chem. Phys. Discuss., 11, 7423–7467, doi:10.5194/acpd-11-7423-2011, 2011.

Virtanen, A., Joutsensaari, J., Koop, T., Kannosto, J., Yli-Pirila, P., Leskinen, J., Makela, J. M., Holopainen, J. K., Pöschl, U., Kulmala, M., Worsnop, D. R., and Laaksonen, A.: An amorphous solid state of biogenic secondary organic aerosol particles, Nature, 467, 824–827, available at: http://www.nature.com/nature/journal/v467/n7317/abs/nature09455.html#supplementary-information, 2010.

Zobrist, B., Marcolli, C., Pedernera, D. A., and Koop, T.: Do atmospheric aerosols form glasses?, Atmos. Chem. Phys., 8, 5221–5244, doi:10.5194/acp-8-5221-2008, 2008.